Geomechanics and Engineering, *Vol. 41, No. 4 (2025) 465-480*
https://doi.org/10.12989/gae.2025.41.4.465

Evaluation of long-term reinforcement of soils using waste brick powder: Insights from strength and characterization

Ahmet Naldan[1a], Harun Akoğuz*[2] and Bülent Çağlar[3b]

[1]*Graduate School of Natural and Applied Sciences, Department of Civil Engineering, Erzincan Binali Yıldırım University, Erzincan, Türkiye*
[2]*Department of Civil Engineering, Faculty of Engineering and Architecture, Erzincan Binali Yıldırım University, Erzincan, Türkiye*
[3]*Department of Food, Feed and Medicine, Institute of Hemp Research, Ondokuz Mayıs University, Samsun, Türkiye*

(*Received October 1, 2024, Revised January 18, 2025, Accepted May 12, 2025*)

Abstract. This study presents an investigation into the reuse potential of waste brick powder (WBP), a cost-effective, environmentally friendly, and easy-to-use waste-based geopolymer for soil improvement as a grouting material. The WBP was obtained by crushing and sieving waste brick to produce the recycled aluminosilicate starting material. Various factors, including liquid-to-solid ratios (1.5, 2.0, and 2.5), NaOH molarities (4, 8, 12, and 16), types of soils, and aging (7, 28, and 365 days), were comprehensively investigated to gain insight into the usability of WBP in soil injection. The effect of alkali-activated waste brick powder (AAWBP) on the mechanical strength and injectability of the soils was assessed, as well as the influence of these factors on the microstructure of samples. The primary structure of AAWBP was determined to be the C-S-H gel, which significantly enhanced the strength development of soil samples. The compressive strength of geopolymer-treated S1, S2, and S3 soil samples reached 4.72, 3.79, and 2.5 MPa after 365 days, respectively, significantly higher than the samples at 28 days (3.32, 1.00, and 0.61 MPa, respectively). Moreover, the strength of samples increased with a decrease in the liquid-solid ratio in all samples, whereas it increased with a rise in the concentration of the activator up to 8 molar for S2 and S3 soil and up to 12 molar for S1 soil. Also, reducing soil particle size positively influenced the development of strength characteristics.

Keywords: alkali activation; geopolymer; ground improvement; injectability; waste brick powder

1. Introduction

Geotechnical engineering is a scientific and technical discipline that is one of the first involved in urban development or infrastructure projects; in many cases, it is the most important (Cardoso 2015). The projects often require enhancing soil properties and mechanical behavior using methods such as horizon lowering, vibrational condensation, dynamic condensation, preloading, and injections to ensure safe construction and operation (Christodoulou *et al.* 2021). Permeation grouting is a low-pressure chemical injection technique that improves soil mechanical properties by creating a solid network in treated material, forming artificially induced cohesion, which binds soil particles without displacing grains during the process (Zullo *et al.* 2020). Portland cement and microfine cement are common cement-based grouts used for permeation grouting and soil stabilization (Bhuiyan *et al.* 2024). The increased use of Portland cement leads to a significant release of carbon dioxide (CO_2) into the atmosphere due to the heating of raw materials during cement manufacturing, which is a major greenhouse gas contributing significantly to global warming (Pavithra *et al.* 2016). Over the past decade, researchers and industry have made significant efforts to reduce CO_2 emissions from cement production and concrete (Dadsetan *et al.* 2019). The global economy's growth is predicted to boost cement production to 5 billion tons annually over the next 30 years, causing rising regulatory and societal pressures to reduce emissions, leading to a surge in demand for alternatives (Hu *et al.* 2021). As alternatives, sodium silicate, polyurethane, acrylamide, aminoplast, epoxy resin, lignosulfonates, phenoplast, and N-methylolacrylamide (NMA), based on the injection of chemical mixtures, are commonly used as grouting materials (Saleh *et al.* 2019). However, these chemical grouting materials, while offering advantages, also have inherent drawbacks, as most of these materials are known to be toxic (Kazemian *et al.* 2010). Organic or toxic solutions are harmful to the environment, and research should focus on using environmentally sustainable materials for soil improvement, particularly in the use of organic or toxic alternatives (Zullo *et al.* 2020).

Green chemistry and technologies are being increasingly recognized for environmental sustainability, shifting from traditional waste perceptions of pollution to treating waste as a resource (Tang *et al.* 2020). The demand for resources worldwide is projected to double by 2050, which requires a more sustainable and judicious use of resources (Belaïd 2022). In recent years, geopolymerization technology has shown significant benefits in reusing various types of waste to create new materials for various purposes (Jelić *et al.* 2023, Pu *et al.* 2024a, b, c). Most waste materials such as building waste, contaminated soil, fly-ash and mine tailings contain large amounts of silica and alumina, which can be used as reagents

*Corresponding author, Assistant Professor
E-mail: hakoguz@erzincan.edu.tr
[a]M.Sc. Student
[b]Professor

ISSN: 2005-307X (Print), 2092-6219 (Online)

for geopolymerization reactions (Van Jaarsveld *et al.* 1997). Geopolymerization is an innovative technique that converts various aluminosilicate materials into useful inorganic polymers or geopolymers (Abdullah *et al.* 2011). Geopolymer technology is considered an optimal solution for recycling construction and demolition waste streams as new value-added products (Tan *et al.* 2022). Major components of the demolition of old buildings include concrete, bricks, mortar, steel, rubble, stone, and timber/wood, particularly in the demolition (Dakwale and Ralegaonkar 2014). Concrete and brick are the primary materials used in construction and demolition waste, resulting from the demolition of old structures, natural disasters, renovations, and the construction of new buildings (Koksal *et al.* 2023). The recovery and reuse of waste clay bricks is crucial for sustainable building environment and resource development, requiring economical and environmentally friendly strategies (Wu *et al.* 2021); therefore, the use of recycled clay bricks from demolition and construction waste is urgently needed for effective utilization (He *et al.* 2021). In addition, waste clay bricks have significant potential as an environmentally friendly and cost-effective raw material for synthesizing geopolymers (Migunthanna *et al.* 2022).

Some studies show that the alkaline solution, the liquid-to-solid ratio (L/S), and aging are key parameters controlling the strength of geopolymer mortars (Huo *et al.* 2021, Naghizadeh and Ekolu 2018). NaOH, Na_2SiO_3, or their combination are the most widely used alkaline activators in the synthesis of alkaline-activated materials (Suwan *et al.* 2023). The alkaline solution appears to influence the properties of the final geopolymer synthesis significantly. For instance, NaOH-based geopolymers have a higher crystallinity than KOH-based geopolymers, which is potentially impacting their mechanical and physical properties (Sore *et al.* 2020). Ilham *et al*. (2021) investigated the synthesis of geopolymers using alkaline molarities (NaOH and KOH) and solid/liquid ratios. They found that the geopolymerization phase increases with NaOH while decreasing with KOH, and the high ratio of solid to liquid produced better geopolymers. Zahid *et al*. (2020) investigated the effects of the geometry of PVA fibers and NaOH molarity (8 M, 12 M, and 16 M) for alkaline solutions to establish mixes of engineered geopolymer composites. The research findings showed that with the increase in the molarity of the NaOH solution, the unconfined compressive strength (UCS) of the mixes has increased; however, using a composite made of 12 M NaOH solution and fine fibers is proposed for an optimally engineered geopolymer matrix. Mustafa et al. (2011) studied the impact of different molarities of NaOH on fly ash geopolymer paste using six different molarities (6, 8, 10, 12, 14, and 16 M) and found that the fly ash-based geopolymer demonstrated high UCS in 7th-day testing with 12 M NaOH concentration but decreased with NaOH solution exceeding 12 M. The molar effect on alkali activation has also been studied by Palomo *et al.* (1999). The results show that a solution of 12M showed faster activation and higher strength compared to a solution of 16 M, and they stated that further investigations on this subject are required. In recent years, numerous studies have investigated the re-utilization of geopolymers in new products.

Previous studies have focused on the preparation of geopolymers and the examination of their mechanical characteristics; however, two research gaps still exist. Firstly, to the best of our knowledge, waste brick powder (WBP) as a geopolymer has not been used for soil improvement with injection techniques. Secondly, existing literature has not thoroughly examined the long-term (365-day) properties of the geopolymer matrix considering the molarities and L/S ratios. This study conducted a series of injection tests to examine the effects of L/S ratio, molarity of alkaline environments, and grain size distribution of soils on strength and injectability. Furthermore, FTIR, TG-DTG, XRD and SEM-EDX were used to analyze the long-term micromechanical structure of the geopolymer matrix. These findings from this research will contribute to a comprehensive database for the eco-friendly and cost-effective application of geopolymer mixtures in practical engineering.

Table 1 Physical property indexes of sand

Group	d_{10} (mm)	d_{30} (mm)	d_{60} (mm)	C_u	C_c	USCS
S1	0.46	0.6	0.74	1.61	1.06	SP
S2	0.95	1.24	1.57	1.65	1.03	SP
S3	2.41	2.63	2.91	1.20	0.99	SP

2. Materials and methods

2.1 Sand

Sand soils were taken from Erzincan, located east of Türkiye, where gravel and sand beds are frequently seen (Özyazıcıoğlu *et al*. 2019). The soils were spread and turned upside down in the laboratory to ensure homogenous drying (air drying) for at least five days and were cleaned for visible impurities. Thereafter, the soils were prepared in uniformly different particle size ranges and labeled in increasing order of grain sizes as “S1”, “S2”, and “S3” (Fig. 1). The main physical property indexes and particle grading curve of soils were determined using ASTM D2487 (ASTM D2487, 2011) criteria, as presented in Table 1 and Fig. 1, respectively. According to the Unified Soil Classification System (USCS), sand can be classified as well-graded sand (SW) if the uniformity coefficient (C_u) is greater than 6 and the curvature coefficient (C_c) ranges between 1 and 3. Sand soils that do not meet either or both of these criteria are classified as poorly graded sand (SP). The soils used in this study were classified as SP, as these did not meet both criteria for SW. The uniform SP soils were used with similar relative densities (D_r = 45–55%) to investigate the effect of grain size on the improvement.

2.2 WBP and alkaline activator

In this study, waste brick was obtained from demolition debris residuals. Because the brick waste particles were relatively large, they were crushed into smaller pieces by a crusher, and brick powder grains less than 75 μm were selected following pulverizing and sieving (Ortega *et al.*

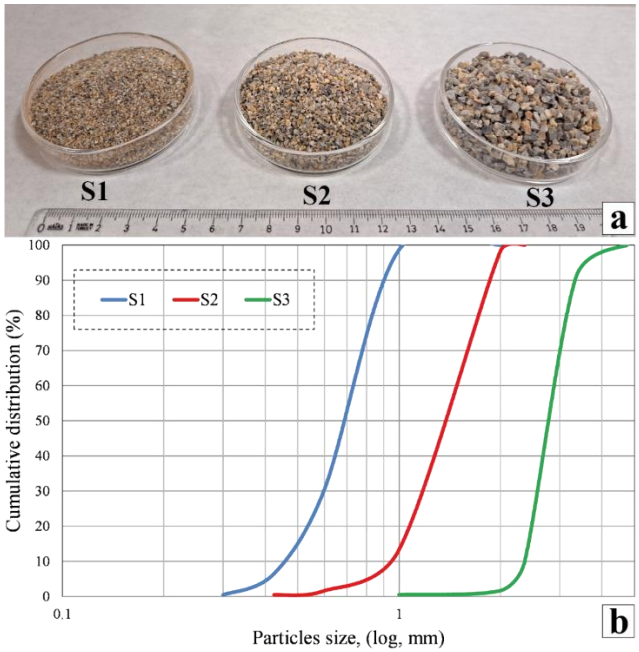

Fig. 1 Properties of sand soils: (a) Visual appearances of sand soils and (b) Grain size distributions of sand soils

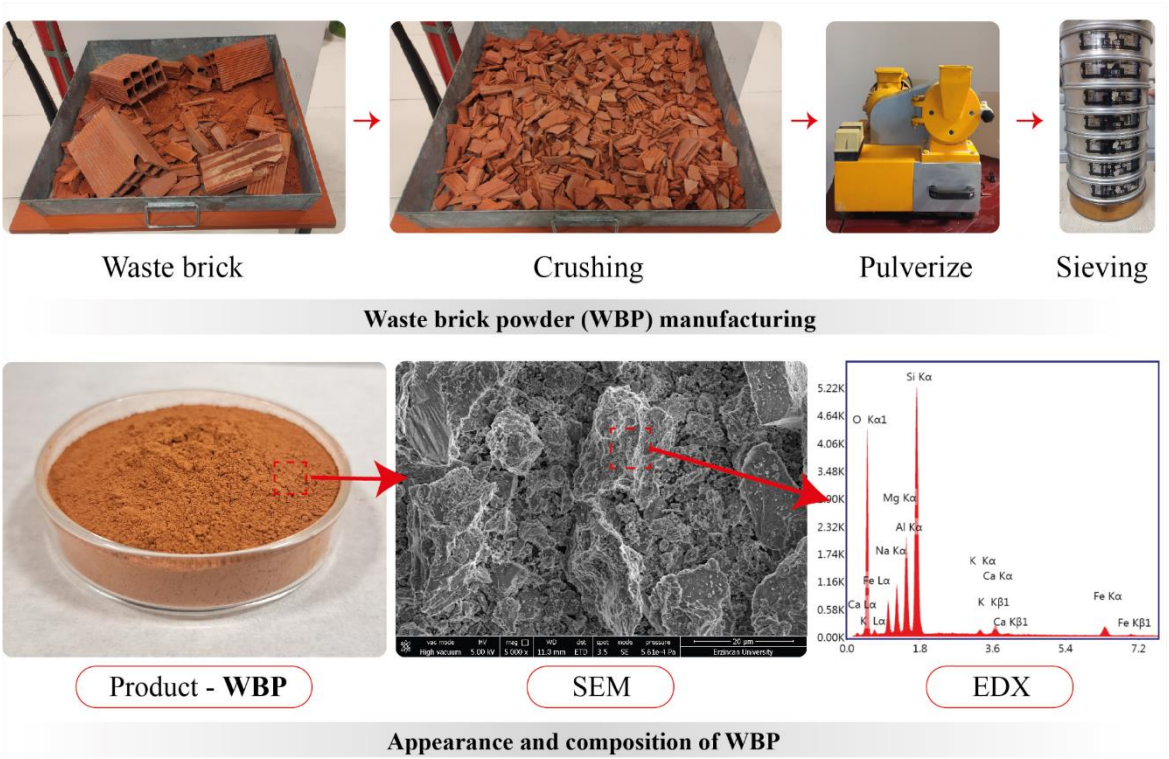

Fig. 2 Manufacturing and composition of WBP

2018). The EDX chemical analysis results (weight and atomic percentages) and the scanning electron microscope (SEM) images of brick waste powder are presented in Table 2 and Fig. 2, respectively. In order to evaluate the characteristics of the injectability of waste brick powder solution, the effect of the liquids to solids (L/S) ratios (1.5, 2, and 2.5) was investigated by injecting the grout. To achieve these ratios, approximately 66.67 g, 50 g, and 40 g of waste brick powder were added for each 100 mL of NaOH solution for L/S ratios of 1.5, 2, and 2.5, respectively, and the mixture was stirred until adequate homogeneity was obtained.

This study used commercially available NaOH flakes (Sigma-Aldrich, ≥98%) as an alkali activator. The NaOH flakes were dissolved in distilled water and kept in a flask. The key point is to make sure the solution contains a

Table 2 EDX analysis results of WBP

Element	O	Na	Mg	Al	Si	K	Ca	Fe
Weight (%)	45.52	5.53	5.35	10.27	26.91	0.6	1.72	4.1
Atomic (%)	59.56	5.04	4.61	7.97	20.06	0.32	0.9	1.54

Table 3 Designed experimental procedures

Soil	Proportion (NaOH solution/waste brick)	NaOH concentrations (molar)	Curing time (day)
S1	1.5, 2, 2.5	4, 8, 12, 16	7, 28, 365
S2	1.5, 2, 2.5	4, 8, 12, 16	7, 28, 365
S3	1.5, 2, 2.5	4, 8, 12, 16	7, 28, 365

suitable amount of NaOH for the reaction to polymerization of geopolymer binders. Therefore, the molarity of NaOH was used at 4, 8, 12, and 16 M levels, as in previous literature research (Ghadir and Ranjbar 2018, Mustafa *et al.* 2012), to determine the effects of alkali activator concentrations on improvement clearly.

2.3 Specimen preparation

PVC molds with a 38-mm inner diameter and 150-mm height were used in this experiment for specimen preparation. According to the target dimension (38 mm in diameter, 76 mm in height), sand soil is placed with a relative density of about 45–55% for tests based on the specific gravity and initial void ratio of sand. To avoid the possible segregation of the prepared soils, causing a change in particle distribution, soil samples were placed into the molds in three equal layers. Having placed the final layer, the molds were closed using hot silicone on both ends with laser-cut plexiglass caps (10 mm in height) with holes for injection inflow, manometer, and outflow. Before injection, the soil sample was filled with water for saturation, and then the outlets of the molds were sealed to control any air bubbles that came out of the inlet and outlet of the molds. After that, the soil samples were set aside until the experiments.

2.4 AAWBP-grouting

The injection test equipment is mainly composed of a manometer, an injection beaker, and a peristaltic pump with the relevant fittings. The injection set-up details are presented in Fig 3. The peristaltic pump, capable of adjusting the injection speed, was used for AAWBP mixtures to be poured into the mold. The injection flow rate of the peristaltic pump was adjusted to 5 ml/min because that was the mean value for the adjustable pump. However, further research may be required to investigate the effect of flow rate on the improvement of soils by using various flow rates. A silicone hose was utilized to inject AAWBP mixtures between the peristaltic pump and mold. The 200 ml of AAWBP mixtures were injected into the mold from the inlets that passed over in the sand column and flowed out of the outlets from the mold during the injection

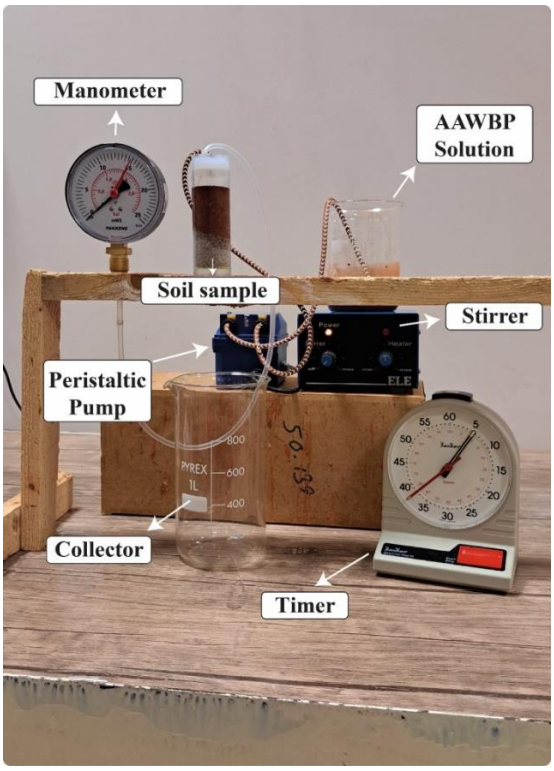

Fig. 3 The experimental details of injection

process. The outlet of mixtures from mold was carried out by using a hole in the bottom of the sand specimen. The increases in pressure caused by injection over time during the experiment were recorded with a manometer through the hole in the upper part of the mold. In their study, Sakr *et al.* (2016) used 1.5 bar pressure for grout during all test series because the higher pressure (5 bar) made the sand collapse and rise above. Therefore, the AAWBP mixture injection was stopped when the manometer reached 1.5 bar pressure. Finally, the injected AAWBP specimens were removed from the PVC molds after 2-3 days and then cured for 7, 28, and 365 days at room temperature.

In the present study, the injection experiments were performed by coupling four operations parameters, including different particle size ranges of soils, concentrations of alkali activator, curing times, and liquid/solid (L/S) ratios of mixtures. These designed experiment procedures are given in Table 3. The conditions for reinforcement of sand with AAWBP mixtures are represented by the sample number SaLbMcDd: “a” means the label of soil, “b” symbolizes the L/S ratio, “c” describes the molarity of the NaOH solution, and “d” illustrates the curing time (days) of the sample.

2.5 Sample preparation for analysis

The microstructure analyses, i.e., XRD, FTIR, TG-DTG, were carried out on WBP and long-term (365-day) AAWBP. The AAWBP binders were collected for analysis after the UCS test from S1 specimens because the highest strength results were obtained from these soil samples. The obtained samples were washed in a falcon tube at least three times

Fig. 4 Preparation of samples for analysis

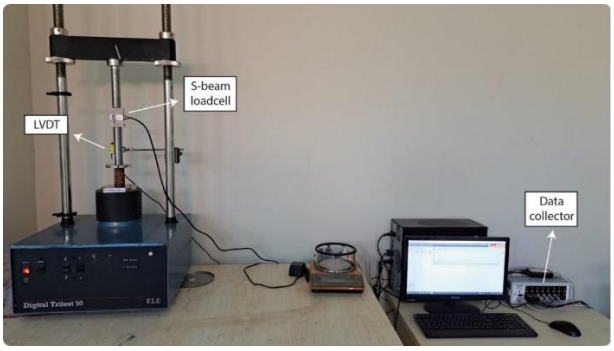

Fig. 5 Experimental details for UCS tests

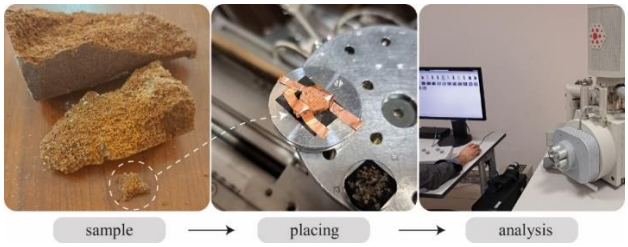

Fig. 6 Specimen preparation for SEM-EDX analysis

with distilled water to remove pollutants using a vortex and centrifuge. Thereafter, the washed samples were centrifuged at 3000 rpm for 1 minute to separate the sample with pure water and put in the oven to ensure the samples were completely dry. Finally, the oven-dried samples were placed in airtight tubes. This method can ensure that different parameters are examined more effectively. The sample preparation processes are illustrated in Fig. 4.

2.6 Unconfined compressive strength (UCS)

In this study, an existing universal testing machine (Fig. 5) was used to carry out UCS on cured sand specimens, with the maximum stress of each test recorded at a constant rate of 1.0 mm/min according to ASTM D2166.

2.7 X-ray diffraction (XRD)

The mineralogical composition of specimens was measured using XRD analysis by a Panalytical Empyrean diffractometer. XRD patterns were obtained between 2° and 90° 2θ at a scan speed of 2° 2θ/min.

2.8 Fourier transform infrared spectroscopy (FT-IR)

FTIR spectrometer analysis was performed using a Thermo Scientific Nicolet 6700 spectrometer to record the infrared spectra of WBP before and after alkali activation with an ATR accessory in a frequency range between 400 cm^{-1} and 4000 cm^{-1}. After scanning, the collected spectrum data was analyzed using the OMNIC software.

2.9 Thermal analysis (TG/DTG)

Thermal analysis curves (TG and DTG) were taken using a PYRIS Diamond TG/DTG apparatus in a dynamic nitrogen gas atmosphere from room temperature to 850 °C at a heating rate of 10°C min^{-1} to evaluate the thermal stabilities of WBP and AAWBP binders.

2.10 Scanning electron microscopy (SEM), Energy dispersive X-ray detector (EDX)

The morphological and structural characterization of binder agents was acquired by using SEM analysis with a QUANTA FEG 450 scanning electron microscope. The EDX analysis was also carried out to clarify the observed structures at their corresponding keV values of elements. The preparation of specimens for SEM-EDX analysis is presented in Fig. 6.

3. Results

3.1 Unconfined compression tests

The compressive strength characteristics of soils being substituted by geopolymer binder were examined under different parameters at 7, 28, and 365 days of age, as presented in Fig. 7. The UCS ranged from 0.09 to 4.72 MPa, 0.02 to 3.79 MPa, and 0.04 to 2.5 MPa for S1, S2, and S3 soils, respectively. The highest UCS value was obtained in 365 days of aging samples with L1.5M12, L1.5M8, and L1.5M8 ratios for S1, S2, and S3 soils, respectively. The results of the present study show that the particle size of soils influenced the development of strength characteristics, as the particle size effect of soils was confirmed by strength results increasing with smaller particle sizes of soils (Lee *et al.* 2019, Xiao *et al.* 2023).

Increasing the molar ratio in the AAWBP solution had a significant impact on the UCS of the samples under the condition of specimens aged 365 days. With an increase to 8M NaOH in the AAWBP solution, it showed a 227%, 282%, and 362% higher mean UCS compared to the 4M group for S1, S2, and S3 soils, respectively. The trend

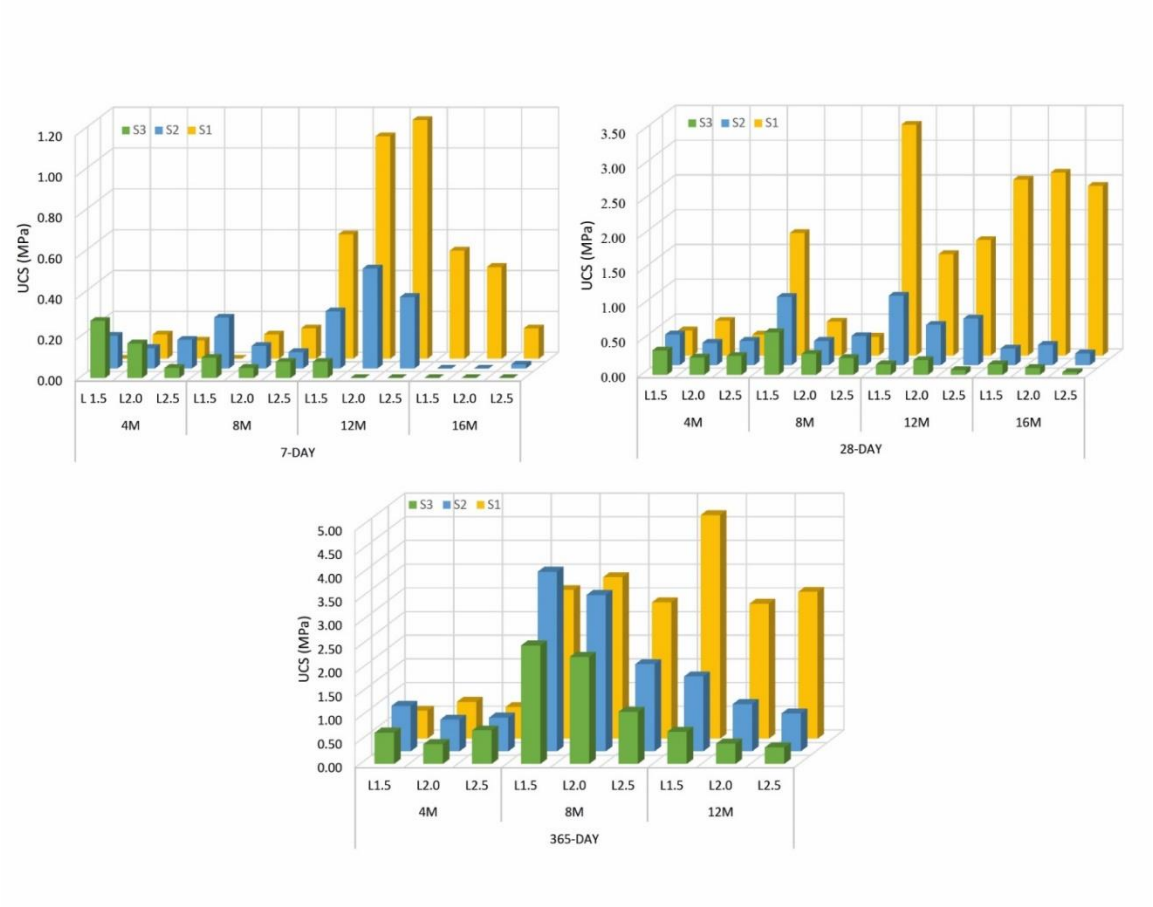

Fig. 7 UCS test results

observed between 8 and 12M UCS is different from that of the between 4 and 8M results, as the strength decreased 62%, 75% for S2 and S3 soils with an increase in NaOH molar from 8 to 12, respectively. At 8M, S2 and S3 soil showed the highest UCS results, whereas at 12M, S1 soil demonstrated the highest UCS, exceeding in 8M samples by about 13%. However, the strength development continued until 12 M and reversed when the molar increased to 16 for S1 soil. Álvarez-Ayuso *et al*. (2008) stated in their research that higher UCS values, except for one geopolymer sample, were observed at 12 M NaOH solutions (5, 8 and 12 M used in their study) as activation media. Alzeebaree et al., (2021) also stated that the UCS of alkali-activated mortar specimens increased up to 12 M NaOH concentration; however, the molarity concentrations increased to 14 or 16 negatively influenced the UCS results. This indicates that more than 12 M alkali dosages negatively influenced the strength characteristics of geopolymers, which is also in good agreement with the UCS results of this study. In another study, Görhan and Kürklü (2014) used 3, 6, and 9 M NaOH for an alkali environment and found that the highest compressive strength of geopolymer mortars was in 6 M samples. It was understood that an excessive or insufficient amount of alkali negatively impacts the setting and hardening of geopolymer paste (Singh *et al*. 2023). Studies in literature have shown that both 8M and 12M NaOH solutions lead to optimal strength development (Ibrahim *et al*. 2022, Jeeva Chithambaram *et al*. 2019, Pratap *et al.* 2023, Zia ul haq *et al.* 2023). However, when considering long-term UCS results in our study, the 12M NaOH solution exhibited optimal strength only for the S1 soil, while the best results for the S2 and S3 soils were achieved with the 8M. In addition, for S1 soil, although notable differences in peak strength values were observed at 12M, the average UCS values for the 8M and 12M solutions were 3.23 MPa and 3.55 MPa, respectively. In their study, Ibrahim *et al*. (2022) examined the strength development of a fly ash/dolomite-based geopolymer with different molarities (6M, 8M, 10M, 12M, and 14M) and determined the optimum NaOH concentration to be 8M.

The study also highlighted that when 8M NaOH was used, elements such as Si, Al, Ca, Mg, and Fe were clearly formed, and the geopolymer exhibited a more homogeneous distribution with fewer unreacted components. Similarly, in our study, while the use of a 12M NaOH concentration provided optimal results for only S1 soil, using an 8M NaOH concentration demonstrated more homogeneous strength development in almost all soil types. In addition, Zivica *et al*. (2015) stated that high doses of activator concentration entail higher costs, and economic factors should not be overlooked. Therefore, it was concluded that the use of 8M NaOH as the alkaline environment concentration may be more effective for long-term strength development.

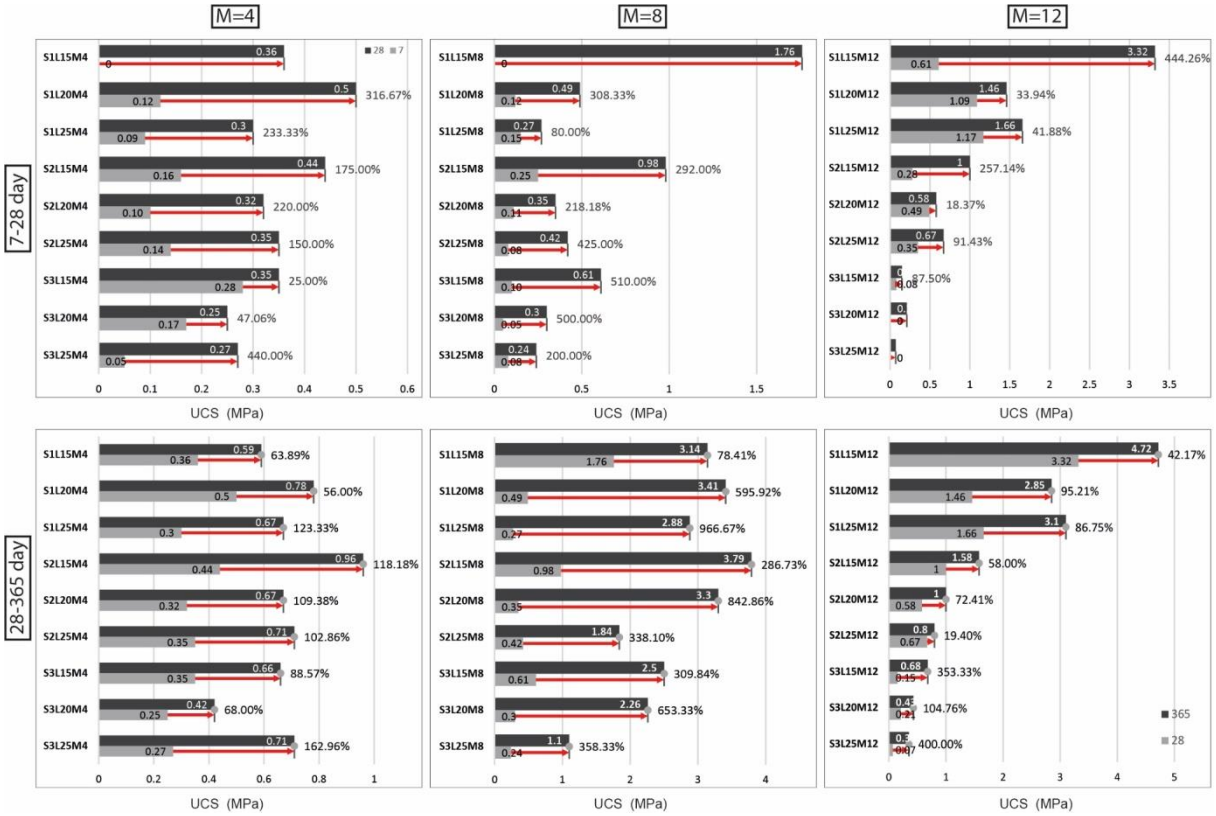

Fig. 8 Strength development of geopolymer treated samples

The determination of the L/S ratio is extremely crucial for geopolymer materials, especially in terms of their application issues (Marczyk *et al.* 2022). The results of this study revealed notable decreases for long-term (365-day) samples in strength as L/S increased from 1.5 to 2.5; that is, UCS decreases of mean 10%, 42%, and 32% were found for S1, S2, and S3 soils, respectively. Additionally, similar circumstances were observed in the early stages (7 and 28 days) of the strength characteristics of the samples. Therefore, it is concluded that increasing the liquid/solid ratio of AAWBP binder leads to an excess of water, which reduces the alkali concentration of activators, which in turn reduces compressive strength (Karakoç *et al.* 2013, Reig *et al.* 2013, Tuyan *et al*. 2018). Nevertheless, as shown in Fig. 8, some samples exhibited higher percentage strength increases despite higher L/S ratios. Consequently, Fig. 7 shows that, for most of the samples, the presence of excess water reduced the alkali concentration, resulting in higher 365-day strength values at lower L/S ratios.

Long-term performance is important for understanding the evolutionary mechanism and the sustainable use of the method in soil improvement. However, long-term monitoring for ground stabilization is still missing (Verma *et al.* 2021). This study provides practical results for the long-term performance mechanism for applications such as field experiments. Based on the findings of early-stage results in this study with the previous literature research, we used 4, 8, and 12M for alkali environments to evaluate the long-term strength characteristics of soils. It was indicated that the curing age played a critical role in developing strength. Regardless of the molar and L/S ratio of AAWBP, it is noticed that the UCS of all samples enhances with the gain of curing age, as seen in Fig. 8. Considering the mean increase of all samples with the increment in the curing age, the UCS showed a trend of rapid growth in the early stage (7 to 28 days) as 222% and slower growth in the long term (28 to 365 days) as 243%. Compared the UCS results with consideration of L/S of the alkali environments, the mean UCS of L/S 1.5 was enhanced over L/S 2 and 2.5 in the short term, while in the long term, a lower increase in UCS was observed in L/S 1.5 than in L/S 2.0 and 2.5, which can be explained by the water content. Yun *et al.* (2018) mentioned that using excessive amounts of water to dilute the alkali activators might reduce the strength capability. In addition, Yang *et al.* (2012) also stated that excess water reduces alkali activation speed and increases setting time. It is understood that excess water in the alkaline environment can cause the reaction to continue in the long term but eventually lead to lower strength.

It was observed that the molars of alkali environments also influence the strength of early-stage and long-term samples. The results indicate that the mean strength between 7 and 28 days (early strength) of 4, 8, and 12M increased by 179%, 282%, and 108%, respectively. On the other hand, aging between 28 and 365 days of samples increased the UCS of specimens 4, 8, and 12M by 99%, 492%, and 137%, respectively. Yomthong *et al*. (2021) investigated the effects of varying NaOH concentrations (ranging from 4M to 12M in 2M increments) on the strength development of geopolymers. They found that

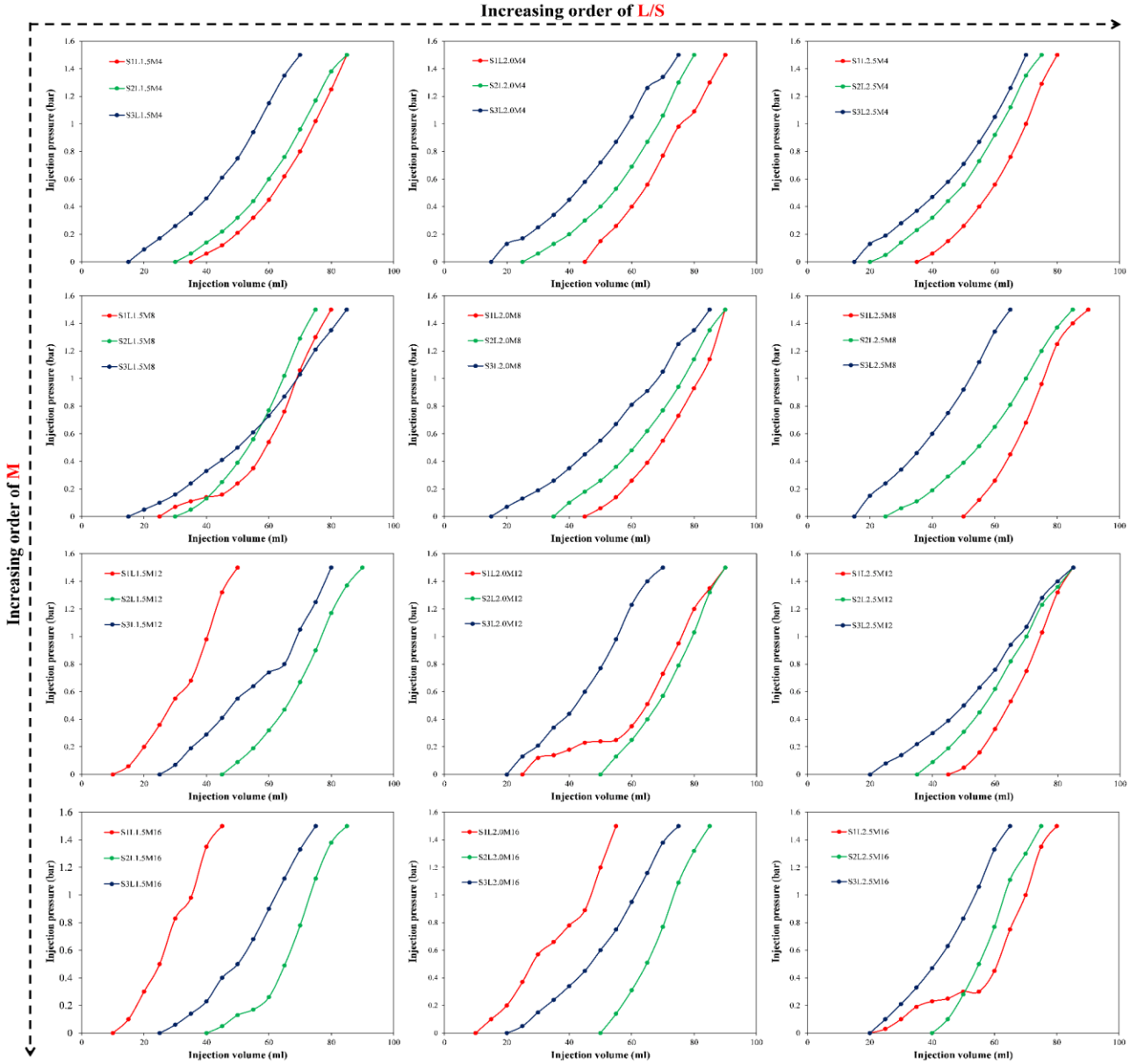

Fig. 9 Injectability results of AAWBP binder

geopolymers with 4M NaOH exhibited low compressive strength due to the insufficient availability of silicate and aluminate species for geopolymerization. However, increasing the NaOH concentration to 8M, 10M, and 12M significantly enhanced the dissolution of these species, accelerating the geopolymerization process and resulting in geopolymers with higher compressive strength. In the present study, the compressive strength of 4M geopolymer samples exhibited a significant increase of 179% when the curing period was extended from 7 to 28 days (early stage). However, as the curing period was further prolonged from 28 days to 365 days (long-term), the compressive strength continued to rise but at a slower rate, with an increase of 99%. Although this represents a substantial gain, the increase observed during the long-term curing phase was notably lower compared to the rapid strength development observed in the early stages. This behavior suggests that most of the geopolymerization occurred within the first 28 days, with minimal further enhancement occurring thereafter. The limited long-term strength development in 4M samples may be attributed to the insufficient availability of reactive silicate and aluminate species, which are crucial for continued geopolymerization. This observation is consistent with previous studies, which reported that lower NaOH concentrations lead to slower and less pronounced strength development due to a similar reduction in available reactive species for geopolymerization. In contrast, when the NaOH concentration was increased to 8M and 12M, a marked difference was observed in the 365-day compressive strength, which surpassed that of the 28-day samples, indicating continued strength development during the long-term curing period. The enhanced dissolution of silicate and aluminate species in the presence of higher NaOH concentrations facilitated the acceleration of the

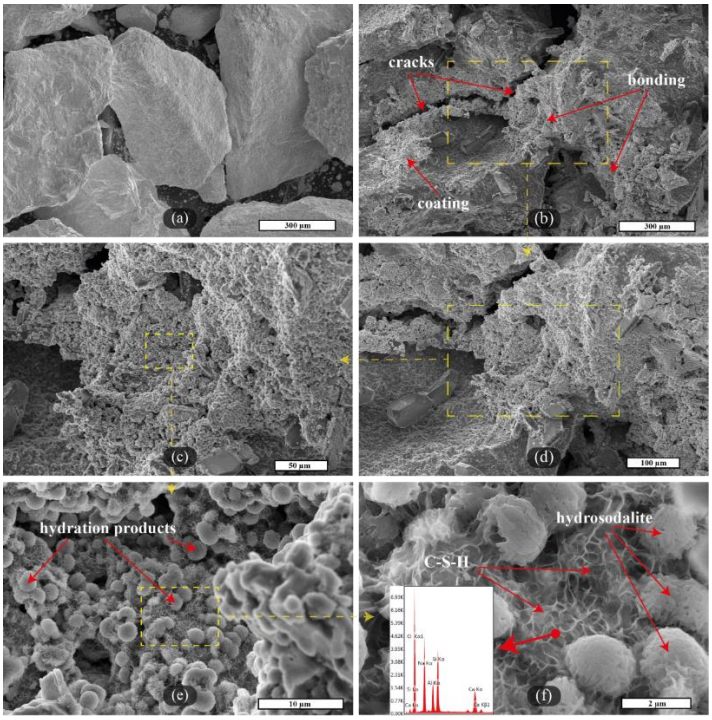

Fig. 10 SEM-EDX analysis results (a) untreated S1 soil (300x), (b) treated S1 soil (300x), (c) 1200x, (d) 600x, (e) 10 000x and (f) 40 000x

geopolymerization process, thereby promoting further strength gain over time. These findings align with those of prior research, which demonstrated that increasing NaOH concentrations results in higher compressive strengths. Moreover, the long-term analysis in this study, supported by FTIR and XRD results, confirms the relationship between higher NaOH concentrations and improved geopolymerization, leading to better strength development over time.

3.2 Injectability properties of AAWBP binder

The W/C ratio is a crucial parameter and significantly influences the injection process and soil improvement, requiring optimal selection for practical applications (Saada *et al.* 2006). Also, the flow of the geopolymer mortar is influenced by the concentration of NaOH and the amount of brick powder utilized (Wong *et al.* 2020). In this section, in order to estimate the injectability of AAWBP, the effects of the L/S ratio in grout, the molarity of the alkali activator (NaOH), as well as the grain size of the soil, have been investigated in model tests. The goal is to develop an approach for injection that is environmentally friendly and can be handled without special equipment. The tests show that the AAWBP solution is injectable to penetrate the grout between the soil grains. WBP has a grain size lower than 0.075 mm, while the grain size range of S1, S2, and S3 soils varied between 0.3 and 1 mm, 0.425 and 2 mm, and 1.0 and 4.75 mm, respectively. The maximum particles of WBP were approximately 4–13 times less than the minimum particle size of soils (S1, S2, and S3). The particle size of WBP could be positively effective to penetrate in micro voids of sand soils by increasing the penetration capacity or injectability of AAWBP. The injection was achieved successfully in all soil types with AAWBP binder; however, the injectability was influenced by the varied parameters used.

The injectability results of the geopolymer binder are presented in Fig. 9. In general, the injection volume of AAWBP has been affected closely by the molarity, grain size distributions, and L/S ratios. As the molarity increased, the injected volume for S1 soil with an L/S ratio of 1.5 and 2.0 decreased by 40 and 45 ml, respectively. In addition, the injected volume for S1 soil is about the same for an L/S ratio of 2.5, with an increase in molarity. On the other hand, as the molarity increased, the difference in injected volume was smaller for S2 and S3 soils compared to S1 soil. Furthermore, considering all influencing factors, the standard deviations of the solution volumes applied to S1, S2, and S3 soils were determined to be 16.7 ml, 5.8 ml, and 7.4 ml, respectively. It is clearly understood that injectability is much more complex in S1 soil than in S2 and S3 soils. The similar standard deviations of the solution volumes for the two soils (S2 and S3) indicate that the measured data can be used to make decisions and provide insights for relevant applications.

The increase in molarity, or L/S ratio, especially affected the injectability of S1 soil. In this case, it is understood that the grain size of soils can be decisive in choosing the L/S ratio and molarity in soil environments, consistent with the observations of Hassanlourad *et al.* (2014). In their study, they conducted an experimental investigation to evaluate the groutability potential of sandy-silty soils using sodium silicate as a chemical grout. Their analysis revealed that soil particle size is the most critical parameter for groutability, compared to other factors such as soil compaction, relative

density, and grout concentration. Moreover, they concluded that as particle size decreases, groutability is significantly affected, with the influence of other parameters being secondary and strongly dependent on particle size. Similarly, in our study, the effect of other parameters on the injectability of the AAWBP solution varied, particularly depending on the soil particle size. Namely, at lower molarities (4M and 8M), S1 soil required the highest injection volume, resulting in longer injection times compared to S2 and S3 soils. However, at higher molarities (12M and 16M), decreasing the L/S ratio had a significant impact, particularly in S1. Under these conditions, the injection volume further decreased, leading to even shorter injection times for S1 compared to S2 and S3. This highlights that higher molarities and lower L/S ratios enable more efficient injections by reducing the volume of AAWBP solution required, particularly in finer-grained soils. Considering the minimum injection volume of AAWBP and injection time, an optimal L/S ratio is proposed for S1, S2, and S3 soils of 1.5, 1.5, and 1.5 or 2.5, respectively. To enhance injectability in the soil environment and be more suitable for all sand soils, a reasonably low L/S ratio (1.5) was also recommended, considering the UCS test results. In addition, SEM analysis results are in good agreement with the experimental results of injectability, which indicates the usefulness of the method.

3.3 SEM results

The SEM analysis was performed after 365 days of curing to evaluate the microstructure of the geopolymer. The SEM images of the S1L1.5M12D365 sample are shown in Fig. 10, which obtained the highest strength of all samples. Moreover, the microstructure of untreated soil is also shown for comparison in Fig. 10(a). SEM images show that at 500x magnification, the AAWBP forms a large accumulation between and on the surface of the soil particles. In addition, as shown in Fig. 10(b), the transgranular cracks observed as a result of the UCS tests are consistent with the findings reported in the literature (Chen *et al*. 2018). At 40 000x magnification, SEM images can identify the bridge structure between the particles. The mechanism of AAWBP was explained clearly by SEM images with magnifications from both overall and regional perspectives.

The untreated soil sample of S1 at 300x magnification is illustrated in Fig. 10(a). As shown in Fig. 10(b), AAWBP gel filled the pores between soil particles and caused the soil particles to aggregate. As illustrated in Fig. 10(e), a large amount of hydration product was formed following the alkali activation reaction. The SEM image with 40 000x magnification in Fig. 10(f) clearly showed that hydrosodalite (a crystalline compound) was formed as a hydration product (Statkauskas *et al*. 2023). Also, as shown in Fig. 10(f), the formation of C-S-H was seen at high-rise magnification levels (Maaze and Shrivastava 2023). In addition, Fig. 10(f) shows that the sample has Ca peaks in the EDS spectra, showing the formation of C-S-H, which may greatly improve the strength of the samples (Cong *et al*. 2022). The XRD results also confirmed the presence of C-S-H.

3.4 XRD analysis results

To evaluate the mineralogical composition of WBP and alkali-activated samples after curing for 365 days at room temperature, the powder XRD diffraction analysis technique was carried out, and the powder XRD patterns of WBP and alkali-activated samples are comparatively given in Fig. 11. The comparison of the peak intensities and areas of minerals in the XRD patterns shows that the main crystalline phase of WBP is quartz (Q). It also contains the albite (A) as a secondary mineral as well as calcite (C), hematite (H) and clinochlore (Cln) minerals as small components. The (100), (101), (110), (102), (200), (201), (112), (211), and (203) crystal planes of quartz are observed at 20.90, 26.65, 36.10, 39.60, 42.50, 45.82, 50.12, 60.19, and 68.20 (2θ) values, respectively (JCPDS 46-1045), whereas the (002), (-201), (111), (130), and (002) reflections of albite are detected at 14.54, 22.10, 23.90, 24.29 and 27.92 (2θ) values, respectively (JCPDS No 09-0466) (Sun *et al.* 2023, Yang *et al*. 2012). In addition, the peaks from calcite are located at 30.42 and 41.00 (2θ); the peaks of hematite are positioned at 33.10, 37.00, and 54.01 (2θ); and the peaks from clinochlore are seen at 19.20 and 25.20 (2θ) values, which have quite weak intensity. The alkali activation of WBP with sodium hydroxide resulted in the emergence of a broad peak in the region of 5–10 (2θ) due to the amorphous aluminosilicate phase of the geopolymer and the appearance of new semi-crystalline XRD peaks belonging to calcium silicate hydrate (CSH) and sodium calcium aluminosilicate hydrate (NACSH) species, indicating the formation of a geopolymer matrix including these species. The XRD peaks belonging to CSH are located at 29.40, 42.90, 46.20, and 55.20 (2θ) values, while the XRD peaks from NACSH are detected at 33.60, 36.30, and 41.50 (2θ) values, and the peak intensities from these species were significantly affected by concentrations of NaOH and L/S ratios. The peak intensities of CSH and NACSH species, which was observed in maximum intensities for the S1L1.5M12D365 sample, paralleled the increasing of the amorphous aluminosilicate phase peak. As stated in the literature, calcium silicate hydrate (CSH) species have a positive role in the geopolymerization process by behaving as nucleation sites for the generation and aggregation of amorphous geopolymer gels, which eventually causes the strengthening of the sample and increasing its compressive strength (Zawrah *et al.* 2016). The XRD peaks belonging to CSH species reached a maximum in the S1L1.5M12D365 sample, which is in good agreement with further reported UCS results. The present study clearly shows that the change of the NaOH concentration and L/S ratio significantly influenced the UCS properties of samples with regard to their CSH amounts in the polymeric matrix.

3.5 FT-IR analysis results

In order to verify the formation of geopolymer matrix

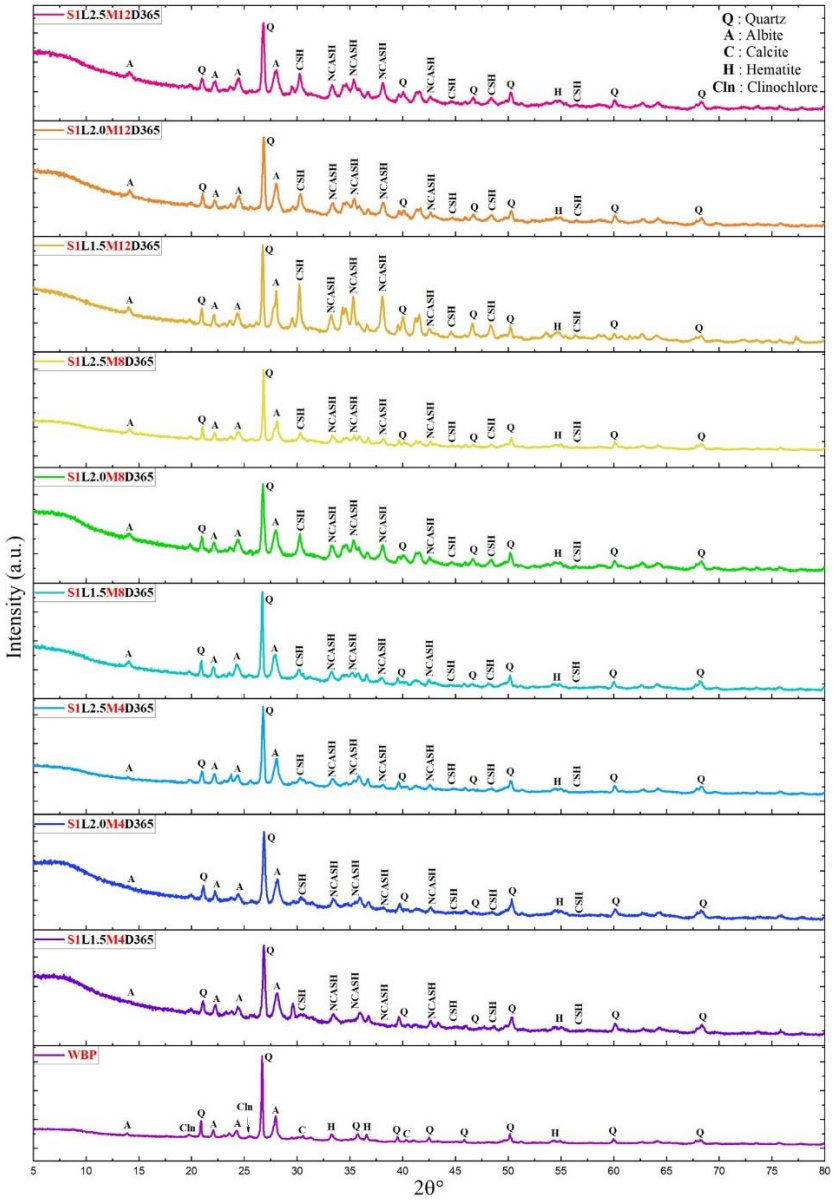

Fig. 11 XRD analysis results

and silicate hydrate species in samples, the ATR-FTIR spectroscopy is performed, which is also a handy technique for identification of chemical species by using vibrational frequencies (Fig. 12). The strong band at 998 cm^{-1} and the shoulder peak at 1048 cm^{-1} are ascribed to the in-plane asymmetric stretching vibrations of Si-O-Si of tetrahedral sheet whereas the IR band in the region of 500-400 cm^{-1} corresponds to deformation vibration of O-Si-O, Al-O-Si and Si-O bonds (Mostafa *et al.* 2009, Shen *et al*. 2022, Zawrah *et al*. 2016). The characteristic IR peaks observed at 795, 777, 693 and 664 cm^{-1} originating from the Si-O-Si bonds (inter tetrahedral bridging) in SiO2 are due to the existence of quartz mineral (Hwang *et al*. 2019, Zawrah *et al*. 2016). After the alkali activation of WBP with sodium hydroxide, the main IR band at 998 cm^{-1} is shifted to lower frequencies in the case of all activated samples as the result of the formation of geopolymer matrix including amorphous aluminosilicate, CSH and NACSH species, which is good agreement with SEM and XRD analysis. This shift in the main IR band, which is related to the emergence in the tetrahedrally placed Al atoms existence in the geopolymer matrix, is gradually changed with the amount of sodium hydroxide and then reached a maximum for the S1L1.5M12D365 sample as an outcome of the formation of CSH and NACSH species (Zawrah *et al*. 2016). This result is consistent with the XRD and UCS results that the NaOH concentration and L/S ratio affected the formation of CSH species in the polymer matrix. Furthermore, the broad OH stretching band around 3600 cm^{-1} and OH bending IR band at 1630 cm^{-1} which belong to water species signifies entrapped water molecules in the large cavities of the polymeric framework of geopolymer product or surface absorbed water (Zawrah *et al.* 2016) There are minor increases in intensity of these OH vibrations due to the

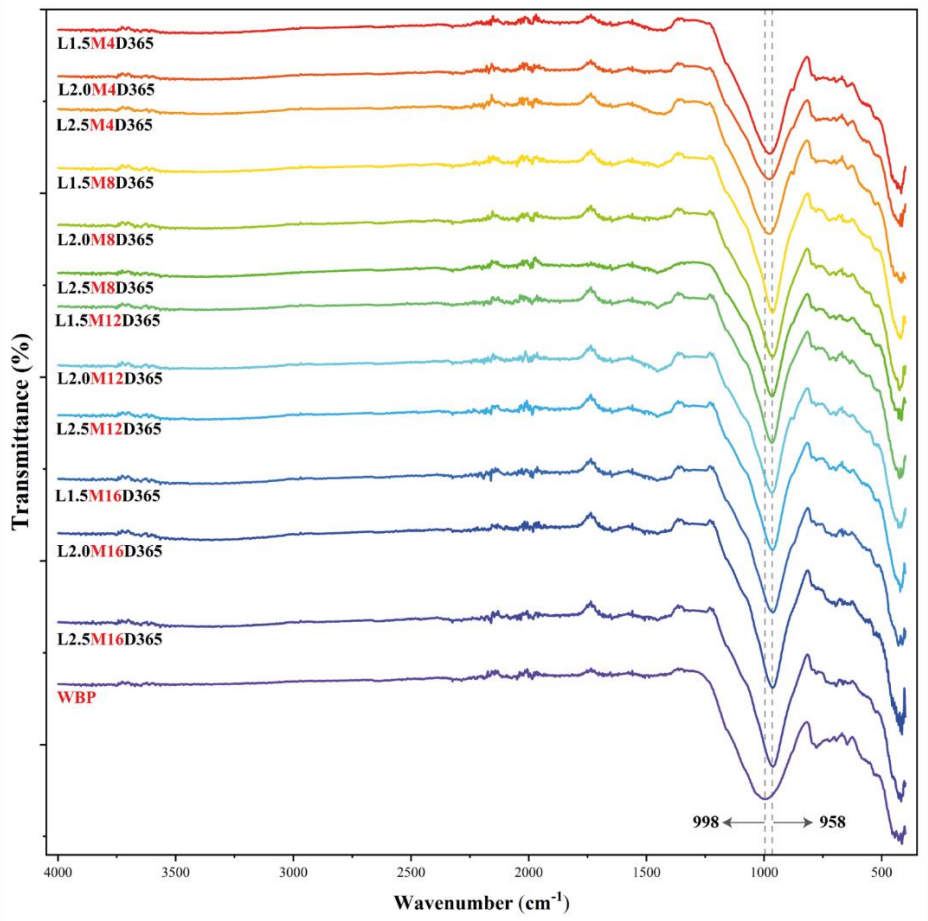

Fig. 12 FT-IR analysis results

formation of hydrated silicate products. What appears to be important in examination of geopolymerization by using IR technique is the shifts and changes in intensity of the IR peak locations, as different amount of the NaOH concentration and L/S ratio are applied. As the silica structures in WB are dissolved by alkali activation and formed the new bonds corresponding to CSH and NACSH species, Si-O-Si peak shifts to lower frequencies whereas the intensities of Al-O-Si and OH vibrations increase in consistent with the fact that formation of sodium calcium aluminosilicate hydrate. However, maintenance of IR bands at 795, 777, 693 and 664 cm^{-1} in the ATR-FTIR spectra of the alkali-modified samples is explained by the presence of undissolved quartz particles, which is in good correlation with the XRD results. In addition, activated samples exhibit the typical stretching vibration of the O-C-O bond at 1420 and 1490 cm^{-1}, which can be assigned to the occurrence of the carbonate mineral owing to atmospheric carbonation (Zawrah *et al.* 2016).

3.6 TG/DTG analysis results

The TG/DTG analysis were applied to evaluate the thermal behaviours of samples depending on mass losses and decomposition temperatures. The TG/DTG curves obtained for the WBP and alkali modified samples were given in Fig. 13. The DTG peak of WBP in the in the temperature range of 520-680°C corresponds to the dehydroxylation of crystalline zeolitic phase whereas the DTG peaks of alkali modified samples determined in the ranges of 30-160°C, 160-400°C, 500-700°C and 720-850°C are attributed to the dehydration of combined free water molecules with CSH species, evaluation of chemical bound water molecules in the geopolymer, NASH and CSH species, the dehydroxylation of crystalline zeolitic phase with decomposition of full CSH species and decomposition of carbonate groups as four-step decomposition process, respectively (Abdel-Gawwad *et al.* 2021, Kumavat *et al.* 2020, Li *et al.* 2022, Rihan Maaze and Shrivastava 2023, Yang *et al.* 2020). The total mass losses of alkali modified samples significantly increased compared to that of the WBP which is associated with the more formation of free and chemical bound water molecules in the geopolymer, NASH and CSH species as well as the formation of carbonate groups by alkali activation. Many researchers agree that the increase in the mass losses in the first three steps shows the more existence of geopolymer and CSH species which led to a noticeable increment of mechanical properties (Cong *et al.* 2022, Li *et al*. 2022). According to the TG/DTG curves, the maximum mass losses was achieved for the S1L1.5M12D365 sample which are consistent with XRD, FTIR, UCS and SEM results.

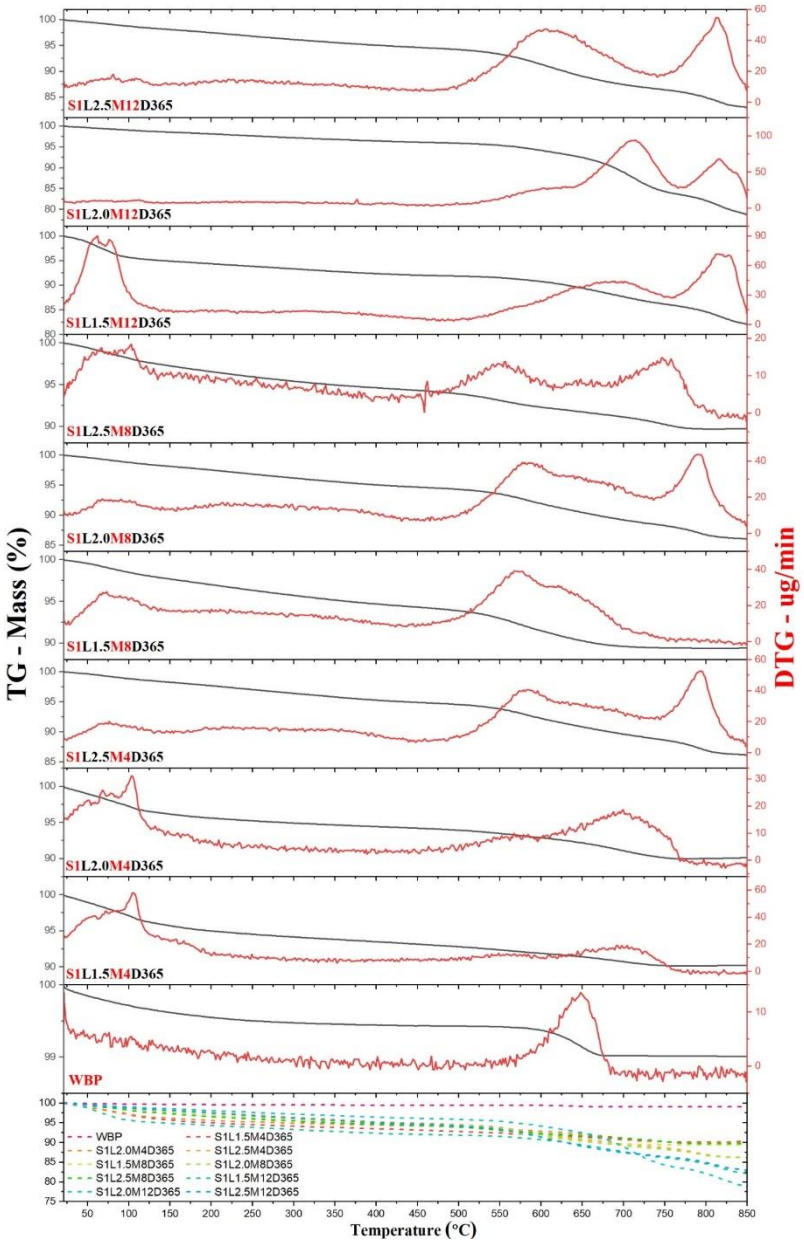

Fig. 13 TG/DTG analysis results

4. Conclusions

This study focused on the waste brick powder as a geopolymer binder to gain insights into the underlying mechanisms and strength properties for their potential use for soil stabilization in long-term applications. The effects of L/S ratios, alkali activator concentration, type of soil, and aging on the microstructure and mechanical properties of geopolymer-treated samples are systematically investigated. The following conclusions can be drawn:

(1) The injectability test results demonstrated that the AAWBP solution is injectable and capable of penetrating the grout between soil grains. WBP, with a grain size smaller than 0.075 mm, was significantly finer than the soil grains (S1, S2, and S3) with sizes ranging from 0.3 to 4.75 mm. This size difference enhanced the injectability of AAWBP, allowing it to penetrate micro voids in the soil. The SEM analysis results also validated the experimental findings, confirming the effectiveness of the method.

(2) The results indicated that AAWBP gel can be used to strengthen soils by causing an alkali-activated reaction that transforms loose and porous soil into a solid structure. The maximum strengths of soil samples were determined to be 4.72, 3.79, and 2.5 MPa for S1, S2, and S3 soils, respectively. The strength results showed that reducing soil particle size positively influenced the development of strength characteristics.

(3) The NaOH concentration of 4 M was found to be inadequate for the strength development of the samples. However, the samples activated with an increased level of 8 M NaOH ultimately achieved strength, indicating sufficient alkalinity for geopolymerization. The strength

increase with increasing NaOH molarity from 8 M to 12 M was observed only in S1 soil samples. In addition, the strength of all samples was negatively influenced when the concentration increased to 16 M. The optimal choice for strength development was found to be 8 M for an alkaline environment, which provided for strength development.

(4) The optimum L/S ratio was determined to be 1.5 for soil samples. A too high L/S ratio adversely affected the geopolymerization of samples because excessive amounts of water decreased the alkali activator concentration, which might reduce the strength capability. Also, the impact of the optimum L/S ratio of 1.5 on strength results at high molarity (8 and 12 M) was much greater than at low molarity (4 M) in an alkaline environment.

(5) The long-term results of AAWBP could be a highly valuable advantage for the evaluation of the lifetime service properties of soil improvement. The UCS of all geopolymer samples increased with the curing time; however, a longer curing time (365 days) significantly promoted compressive strength compared to 28 days of samples. The UCS of geopolymer-treated S1, S2, and S3 soil samples in a long-term increment (28 to 365 days) was determined to be 42%, 279%, and 310%, respectively.

(6) In micro examinations, it was observed that the main reaction product was C-S-H gel. As the samples aged, the gels gradually solidified into the soil and improved the connection of soil particles to form a structure; when the reaction time was prolonged, the network structure got more densified, which resulted in improved UCS of soils.

This study provides a new understanding of waste brick powder geopolymer and broadens its applicability. In future studies, environmental effects such as freeze-thaw and wet-dry, as well as full-scale application, can be considered for better insight into soil improvement by using geopolymerization.

Acknowledgments

This study was produced from the MSc thesis study carried out by Ahmet Naldan under the supervisor of Harun Akoğuz and co-supervisor of Bülent Çağlar at Erzincan Binali Yıldırım University, Graduate School of Natural and Applied Sciences, Department of Civil Engineering.

References

Abdel-Gawwad, H.A., Rashad, A.M., Mohammed, M.S. and Tawfik, T.A. (2021), "The potential application of cement kiln dust-red clay brick waste-silica fume composites as unfired building bricks with outstanding properties and high ability to CO2-capture", *J. Build. Eng*., **42**, 102479. https://doi.org/10.1016/j.jobe.2021.102479.

Abdullah, M.M.A., Hussin, K., Bnhussain, M., Ismail, K.N. and Ibrahim, W.M.W. (2011), "Mechanism and chemical reaction of fly ash geopolymer cement-a review", *Int. J. Pure Appl. Sci. Technol.*, **6**, 35-44.

Álvarez-Ayuso, E., Querol, X., Plana, F., Alastuey, A., Moreno, N., Izquierdo, M., Font, O., Moreno, T., Diez, S., Vázquez, E. and Barra, M. (2008), "Environmental, physical and structural characterisation of geopolymer matrixes synthesised from coal (co-)combustion fly ashes", *J. Hazard Mater*., **154**, 175-183. https://doi.org/10.1016/j.jhazmat.2007.10.008

Alzeebaree, R., Mawlod, A.O., Mohammedameen, A. and Niş, A. (2021), "Using of recycled clay brick/fine soil to produce sodium hydroxide alkali activated mortars", *Adv. Struct. Eng*., **24**, 2996–3009. https://doi.org/10.1177/13694332211015742.

ASTM D2487 (2011), Standard practice for classification of soils for engineering purposes.

Belaïd, F. (2022), "How does concrete and cement industry transformation contribute to mitigating climate change challenges? *Resour. Conserv. Recy. Adv*., **15**, 200084. https://doi.org/10.1016/j.rcradv.2022.200084.

Bhuiyan, M.R., Masum, S.R., Parvej, M.T. and Sanuwar, S.M. (2024), "An overview of soil improvement through ground grouting", *J. Geosci. Environ. Protect*., **12**, 51-63. https://doi.org/10.4236/gep.2024.121004.

Cardoso, A.S. (2015), "Emerging trends in geotechnical engineering", *Soils Rocks*, **38**, 95-118. https://doi.org/10.28927/SR.382095.

Chen, C.F., Xu, T. and Li, S.H. (2018), "Microcrack evolution and associated deformation and strength properties of sandstone samples subjected to various strain rates", *Minerals*, **8**(6), 231. https://doi.org/10.3390/min8060231.

Christodoulou, D., Lokkas, P., Markou, I., Droudakis, A., Chouliaras, I. and Alamanis, N. (2021), "Principles and developments in soil grouting: A historical review", *WSEAS T. Adv. Eng. Educ*., **18**, 175-191. https://doi.org/10.37394/232010.2021.18.18.

Cong, P., Cheng, Y., Ge, W. and Zhang, A. (2022), "Mechanical, microstructure and reaction process of calcium carbide slag-waste red brick powder based alkali-activated materials (CWAAMs)", *J. Clean Prod*., **331**, 129845. https://doi.org/10.1016/j.jclepro.2021.129845.

Dadsetan, S., Siad, H., Lachemi, M. and Sahmaran, M. (2019), "Construction and demolition waste in geopolymer concrete technology: A review", *Mag. Concrete Res*., **71**, 1232-1252. https://doi.org/10.1680/jmacr.18.00307.

Dakwale, V.A. and Ralegaonkar, R.V. (2014), "Development of sustainable construction material using construction and demolition waste", *Indian J. Eng. Mater. Sci*., **21**, 451-457.

Ghadir, P. and Ranjbar, N. (2018), "Clayey soil stabilization using geopolymer and Portland cement", *Constr. Build. Mater*., **188**, 361-371. https://doi.org/10.1016/j.conbuildmat.2018.07.207.

Görhan, G. and Kürklü, G. (2014), "The influence of the NaOH solution on the properties of the fly ash-based geopolymer mortar cured at different temperatures", *Compos. B Eng*., **58**, 371-377. https://doi.org/10.1016/j.compositesb.2013.10.082.

Hassanlourad, M., Vosoughi, M. and Sarrafi, A. (2014), "Predicting the grouting ability of sandy soils by artificial neural networks based on experimental tests", *Civil Eng. Infrastruct. J*., **47**, 239-253. https://doi.org/10.7508/ceij.2014.02.007.

He, Z., Zhu, H., Zhang, M., Shi, J., Du, S. and Liu, B. (2021), "Autogenous shrinkage and nano-mechanical properties of UHPC containing waste brick powder derived from construction and demolition waste", *Constr. Build. Mater*., **306**, 124869. https://doi.org/10.1016/j.conbuildmat.2021.124869.

Hu, W., Ma, Y., Koehler, M., Gong, H. and Huang, B. (2021), "Mix design optimization and early strength prediction of unary and binary geopolymer from multiple waste streams", *J. Hazard Mater*., **403**, 123632. https://doi.org/10.1016/j.jhazmat.2020.123632.

Huo, W., Zhu, Z., Chen, W., Zhang, J., Kang, Z., Pu, S. and Wan, Y. (2021), "Effect of synthesis parameters on the development of unconfined compressive strength of recycled waste concrete powder-based geopolymers", *Constr. Build. Mater*., **292**, 123264. https://doi.org/10.1016/j.conbuildmat.2021.123264.

Hwang, C.L., Damtie Yehualaw, M., Vo, D.H. and Huynh, T.P. (2019), "Development of high-strength alkali-activated pastes containing high volumes of waste brick and ceramic powders", *Constr. Build. Mater.*, **218**, 519-529. https://doi.org/10.1016/j.conbuildmat.2019.05.143.

Ibrahim, W.M.W., Abdullah, M.M.A.B., Ahmad, R., Sandu, A.V., Vizureanu, P., Benjeddou, O., Rahim, A., Ibrahim, M. and Sauffi, A.S. (2022), "Chemical distributions of different sodium hydroxide molarities on fly ash/dolomite-based geopolymer", *Materials*, 15. https://doi.org/10.3390/ma15176163.

Ilham, D.J., Anggarini, U., Juniarti, J. and Fiantis, D. (2021), "Utilization of volcanic ashes for geopolymer based on alkaline activator and solid-liquid ratio", *IOP Conf. Ser. Earth Environ. Sci.*, **708**, 012058. https://doi.org/10.1088/1755-1315/708/1/012058.

Jeeva Chithambaram, S., Kumar, S. and Prasad, M.M. (2019), "Study on effect of sodium hydroxide concentration on geopolymer mortar, in: (Eds., Das, B.B. and Neithalath, N.), Sustainable Construction and Building Materials. Springer Singapore, Singapore, 651-658.

Jelić, I., Savić, A., Miljojčić, T., Sljivic-Ivanovic, M., Dimović, S., Janković, M., Stanić, V., Zakić, D. and Antonijevic, D. (2023), "Reuse of solid brick waste mix in geopolymerization–a preliminary investigation", *Proceedings of the IRASA International Scientific Conference Science*, Education Technology and Innovation, SETI V 2023 Book of Proceedings. IRASA–International Research Academy of Science and Art Belgrade, 416-422.

Karakoç, M.B., Kantarci, F., Türkmen, İ., Demirboğa, R., Maraş, M.M. and Toprak, M.U. (2013), "Mechanical properties and setting time of geopolymer paste and mortar produced from ferrochrome slag", *Proceedings of the 2013 International Conference on Renewable Energy Research and Applications (ICRERA)*. 52-57. https://doi.org/10.1109/ICRERA.2013.6749725.

Kazemian, S., Huat, B.B.K., Prasad, A. and Barghchi, M. (2010), "A review of stabilization of soft soils by injection of chemical grouting", *Aust. J. Basic Appl. Sci.*, **4**, 5862-5868.

Koksal, F., Bayraktar, O.Y., Bodur, B., Benli, A. and Kaplan, G. (2023), "Insulating and fire-resistant performance of slag and brick powder based one-part alkali-activated lightweight mortars", *Struct. Concrete*, **24**, 3128-3146. https://doi.org/10.1002/suco.202200607.

Kumavat, H.R., Chandak, N.R. and Jadhav, D.J. (2020), "Utilization of clay brick waste powder for partial replacement with cement in cement mortar, (Ed., Bishnoi, S.), Calcined Clays for Sustainable Concrete. Springer Singapore, Singapore, 95-103.

Lee, C., Choo, H., Ku, T. and Lee, W. (2019), "Estimating UCS of cement-grouted sand using characteristics of sand and UCS of pure grout", *Geomech. Eng.*, **19**(4), 343-352. https://doi.org/10.12989/gae.2019.19.4.343.

Li, Y., Shen, J., Lin, H., Lv, J., Feng, S. and Ci, J. (2022), "Properties and environmental assessment of eco-friendly brick powder geopolymer binders with varied alkali dosage", *J. Build. Eng.*, **58**, 105020. https://doi.org/10.1016/j.jobe.2022.105020.

Maaze, M.R. and Shrivastava, S. (2023), "Design optimization of a recycled concrete waste-based brick through alkali activation using Box- Behnken design methodology", *J. Build. Eng.*, **75**, 106863. https://doi.org/10.1016/j.jobe.2023.106863.

Marczyk, J., Ziejewska, C., Pławecka, K., Bąk, A., Łach, M., Korniejenko, K., Hager, I., Mikuła, J., Lin, W.T. and Hebda, M. (2022), "Optimizing the L/S ratio in geopolymers for the production of large-size elements with 3D printing technology", *Materials*, 15. https://doi.org/10.3390/ma15093362.

Migunthanna, J., Rajeev, P. and Sanjayan, J. (2022), "Waste clay bricks as a geopolymer binder for pavement construction", *Sustainability*, **14**, 6456. https://doi.org/10.3390/su14116456.

Mostafa, N.Y., Kishar, E.A. and Abo-El-Enein, S.A. (2009), "FTIR study and cation exchange capacity of Fe3+- and Mg2+-substituted calcium silicate hydrates", *J. Alloys Compd.*, **473**, 538-542. https://doi.org/10.1016/j.jallcom.2008.06.029.

Mustafa, A., Abdullah, M.M.A.B., Kamarudin, H., Binhussain, M., Nizar, K., Razak, R. and Yahya, Z. (2012), "The processing, characterization, and properties of fly ash based geopolymer concrete", *Rev. Adv. Mater. Sci.*, **30**, 90-97.

Mustafa, A., Abdullah, M.M.A.B., Kamarudin, H., Binhussain, M., Nizar, K., Razak, R. and Yahya, Z. (2011), "Microstructure of different NaOH molarity of fly ash- based green polymeric cement", *J. Eng. Tech. Res.*, **3**, 44-49.

Naghizadeh, A. and Ekolu, S.O. (2018), "Effect of mix parameters on strength of geopolymer mortars-experimental study", *Proceedings of the 6th International Conference on Durability of Concrete Structures*.

Ortega, J.M., Letelier, V., Solas, C., Moriconi, G., Climent, M.Á. and Sánchez, I. (2018), "Long-term effects of waste brick powder addition in the microstructure and service properties of mortars", *Constr. Build. Mater.*, **182**, 691-702. https://doi.org/10.1016/j.conbuildmat.2018.06.161.

Özyazicioğlu, M., Dönmezçelik, K., Orhan, S.N. and Özkan, M.Y. (2019), "Erzincan İli Zemin Büyütme Etkilerine Dayalı Mikrobölgeleme Çalışması", *Doğal Afetler ve Çevre Dergisi*, **5**, 247-256. https://doi.org/10.21324/dacd.457438.

Palomo, A., Grutzeck, M.W. and Blanco, M.T. (1999), "Alkali-activated fly ashes: A cement for the future", *Cement Concrete Res.*, **29**, 1323-1329. https://doi.org/10.1016/S0008-8846(98)00243-9.

Pavithra, P., Srinivasula Reddy, M., Dinakar, P., Hanumantha Rao, B., Satpathy, B.K. and Mohanty, A.N. (2016), "Effect of the Na2SiO3/NaOH ratio and NaOH molarity on the synthesis of fly ash-based geopolymer mortar", *Proceedings of the Geo-Chicago*. https://doi.org/10.1061/9780784480151.034.

Pratap, B., Mondal, S. and Hanumantha Rao, B. (2023), "NaOH molarity influence on mechanical and durability properties of geopolymer concrete made with fly ash and phosphogypsum", *Structures*, **56**, 105035. https://doi.org/10.1016/j.istruc.2023.105035.

Pu, S., Shen, Z., Duan, W., Lang, L., Liu, Y., Xu, B., Yao, H. and Mei, G. (2024a), "Discussion on the applicability and mechanism of phosphate-based geopolymers used for cadmium and cadmium-lead heavy metals solidification/stabilization", *J. Environ. Chem. Eng.*, **12**, 113846. https://doi.org/10.1016/j.jece.2024.113846.

Pu, S., Xu, B., Cai, G., Duan, W., Liu, Y., Lang, L., Shen, Z. and Yao, H. (2024b), "Strongly acidic lead contaminated soil solidification/stabilization using metakaolin-modified fly ash phosphoric-based geopolymer", *Chem. Eng. J.*, **496**, 154336. https://doi.org/10.1016/j.cej.2024.154336.

Pu, S., Yao, H., Wu, Z., Cai, G., Duan, W., Wang, A., Wu, J., Li, Y., Xu, B. and Shen, Z. (2024c), "Investigation on the behavior of fly ash phosphate-based geopolymer stabilized acidic lead contaminated soil", *J. Environ. Chem. Eng.*, **12**, 114739. https://doi.org/10.1016/j.jece.2024.114739.

Reig, L., Tashima, M.M., Borrachero, M.V., Monzó, J., Cheeseman, C.R. and Payá, J. (2013), "Properties and microstructure of alkali-activated red clay brick waste", *Constr. Build. Mater.*, **43**, 98–106. https://doi.org/10.1016/j.conbuildmat.2013.01.031

Rihan Maaze, M. and Shrivastava, S. (2023), "Design development of sustainable brick-waste geopolymer brick using full factorial design methodology", *Constr. Build. Mater.*, **370**, 130655. https://doi.org/10.1016/j.conbuildmat.2023.130655.

Saada, Z., Canou, J., Dormieux, L. and Dupla, J.C. (2006), "Evaluation of elementary filtration properties of a cement grout

injected in a sand", *Can. Geotech. J.*, **43**, 1273-1289. https://doi.org/10.1139/t06-082.

Sakr, M.A., Nazir, A.K., Azzam, W.R. and Sallam, A.F. (2016), "Behavior of grouted single screw piles under inclined tensile loads in sand", *EJGE*, **21**, 572-591.

Saleh, S., Yunus, N.Z.M., Ahmad, K. and Ali, N. (2019), "Improving the strength of weak soil using polyurethane grouts: A review", *Constr. Build. Mater.*, **202**, 738-752. https://doi.org/10.1016/j.conbuildmat.2019.01.048.

Shen, J., Li, Y., Lin, H., Lv, J., Feng, S. and Ci, J. (2022), "Early properties and microstructure evolution of alkali-activated brick powder geopolymers at varied curing humidity", *J. Build. Eng.*, **54**, 104674. https://doi.org/10.1016/j.jobe.2022.104674.

Singh, B.K., Kumar, R. and Sengupta, S. (2023), "Industrial production of fly ash and sand-based geopolymer bricks using different molarity of NaOH solution, and assessment of their mechanical and durability properties", *Iran J. Sci. Tech. T. Civil Eng.*, https://doi.org/10.1007/s40996-023-01154-2

Sore, S.O., Messan, A., Prud'Homme, E., Escadeillas, G. and Tsobnang, F. (2020), "Comparative study on geopolymer binders based on two alkaline solutions (NaOH and KOH)", *J. Min. Mater. Character. Eng.*, **8**, 407.

Statkauskas, M., Vaičiukynienė, D., Grinys, A. and Paul Borg, R. (2023), "Mechanical properties and microstructure of ternary alkali activated system: Red brick waste, metakaolin and phosphogypsum", *Constr. Build. Mater.*, **387**, 131648. https://doi.org/10.1016/j.conbuildmat.2023.131648.

Sun, Y., Liu, S., Wen, Q., Guo, J. and Yang, Z. (2023), "Experimental and DFT simulation studies on the mechanism of acid and alkali promoted dissolution of albite", *Appl. Surf. Sci.*, **641**, 158475. https://doi.org/10.1016/j.apsusc.2023.158475.

Suwan, T., Wong, H.S., Fan, M., Jitsangiam, P., Thongchua, H. and Chindaprasirt, P. (2023), "Laboratory-grade vs. industrial-grade NaOH as alkaline activator: The properties of coal fly ash based-alkaline activated material for construction", *Case Studies Constr. Mater.*, **19**, e02427. https://doi.org/10.1016/j.cscm.2023.e02427.

Tan, J., Cai, J. and Li, J. (2022), "Recycling of unseparated construction and demolition waste (UCDW) through geopolymer technology", *Constr. Build. Mater.*, **341**, 127771. https://doi.org/10.1016/j.conbuildmat.2022.127771.

Tang, Z., Li, W., Tam, V.W.Y. and Xue, C. (2020), "Advanced progress in recycling municipal and construction solid wastes for manufacturing sustainable construction materials", *Resour. Conserv. Recy. X*, **6**, 100036. https://doi.org/10.1016/j.rcrx.2020.100036.

Tuyan, M., Andiç-Çakir, Ö. and Ramyar, K. (2018), "Effect of alkali activator concentration and curing condition on strength and microstructure of waste clay brick powder-based geopolymer", *Compos. B Eng.*, **135**, 242-252. https://doi.org/10.1016/j.compositesb.2017.10.013.

Van Jaarsveld, J.G.S., Van Deventer, J.S.J. and Lorenzen, L. (1997), "The potential use of geopolymeric materials to immobilise toxic metals: Part I. Theory and applications", *Min. Eng.*, **10**, 659-669. https://doi.org/10.1016/S0892-6875(97)00046-0.

Verma, H., Ray, A., Rai, R., Gupta, T. and Mehta, N. (2021), "Ground improvement using chemical methods: A review", *Heliyon*, **7**(7). https://doi.org/10.1016/j.heliyon.2021.e07678.

Wong, C.L., Mo, K.H., Alengaram, U.J. and Yap, S.P. (2020), "Mechanical strength and permeation properties of high calcium fly ash-based geopolymer containing recycled brick powder", *J. Build. Eng.*, **32**, 101655. https://doi.org/10.1016/j.jobe.2020.101655.

Wu, J.D., Guo, L.P. and Qin, Y.Y. (2021), "Preparation and characterization of ultra-high-strength and ultra-high-ductility cementitious composites incorporating waste clay brick powder", *J. Clean Prod.*, **312**, 127813. https://doi.org/10.1016/j.jclepro.2021.127813.

Xiao, Y., Xiao, W., Wu, H., Zhao, H. and Liu, H. (2023), "Particle size effect on unconfined compressive strength of biotreated sand", *Transport. Geotech.*, **42**, 101092. https://doi.org/10.1016/j.trgeo.2023.101092.

Yang, D., Liu, M. and Ma, Z. (2020), "Properties of the foam concrete containing waste brick powder derived from construction and demolition waste", *J. Build. Eng.*, **32**, 101509. https://doi.org/10.1016/j.jobe.2020.101509.

Yang, M., Guo, Z., Deng, Y., Xing, X., Qiu, K., Long, J. and Li, J. (2012), "Preparation of CaO–Al2O3–SiO2 glass ceramics from coal gangue", *Int. J. Miner. Process.*, **102-103**, 112-115. https://doi.org/10.1016/j.minpro.2011.11.004.

Yang, T.R., Chang, T.P., Chen, B.T., Shih, J.Y. and Lin, W.L. (2012), "Effect of alkaline solutions on engineering properties of alkali-activated GGBFS paste", *J. Mar. Sci. Technol.*, **20**, 10. https://doi.org/10.51400/2709-6998.1809.

Yomthong, K., Wattanasiriwech, D., Aungkavattana, P. and Wattanasiriwech, S. (2021), "Effect of NaOH concentration and curing regimes on compressive strength of fly ash-based geopolymer", *Mater. Today Proc.*, **43**, 2647-2654. https://doi.org/10.1016/j.matpr.2020.04.630.

Yun, L.H., Leong, O.D.E., G, S.J. and Ali, N. (2018), "Strength development of soil–fly ash geopolymer: Assessment of soil, fly ash, alkali activators, and water", *J. Mater. Civil Eng.*, **30**, 04018171. https://doi.org/10.1061/(ASCE)MT.1943-5533.0002363.

Zahid, M., Shafiq, N., Razak, S.N.A. and Tufail, R.F. (2020), "Investigating the effects of NaOH molarity and the geometry of PVA fibers on the post-cracking and the fracture behavior of engineered geopolymer composite", *Constr. Build. Mater.*, **265**, 120295. https://doi.org/10.1016/j.conbuildmat.2020.120295.

Zawrah, M.F., Gado, R.A., Feltin, N., Ducourtieux, S. and Devoille, L. (2016), "Recycling and utilization assessment of waste fired clay bricks (Grog) with granulated blast-furnace slag for geopolymer production", *Process Saf. Environ. Protect.*, **103**, 237-251. https://doi.org/10.1016/j.psep.2016.08.001.

Zia ul haq, Md., Sood, H., Kumar, R., Chandra Jena, P. and Kumar Joshi, S. (2023), "Optimizing the strength of geopolymer concrete incorporating waste plastic", *Mater. Today Proc.*, https://doi.org/10.1016/j.matpr.2023.08.214.

Zivica, V., Palou, M. and Križma, M. (2015), "Geopolymer cements and their properties: A review", *Build. Res. J.*, 61. https://doi.org/10.2478/brj-2014-0007.

Zullo, R., Verdolotti, L., Liguori, B., Lirer, S., Salzano de Luna, M., Malara, P. and Filippone, G. (2020), "Effect of rheology evolution of a sustainable chemical grout, sodium-silicate based, for low pressure grouting in sensitive areas: Urbanized or historical sites", *Constr. Build. Mater.*, **230**, 117055. https://doi.org/10.1016/j.conbuildmat.2019.117055

CC